

Endogenous or Exogenous Retinal Pigment Epithelial Cells: A Comparison of Two Experimental Animal Models of Proliferative Vitreoretinopathy

Chee Wai Wong¹⁻³, Joanna Marie Fianza Busoy², Ning Cheung¹⁻³,
Veluchamy Amutha Barathi², Gert Storm^{4,5}, and Tina T. Wong¹⁻³

¹ Singapore National Eye Centre, Singapore

² Singapore Eye Research Institute, Singapore

³ Duke–NUS Graduate Medical School, Singapore

⁴ Department of Pharmaceutics, Utrecht Institute for Pharmaceutical Sciences, Utrecht University, Utrecht, The Netherlands

⁵ Department of Experimental Molecular Imaging, University Clinic and Helmholtz Institute for Biomedical Engineering, RWTH Aachen University, Aachen, Germany

Correspondence: Tina T. Wong, Singapore National Eye Centre, 11 Third Hospital Avenue, 168751, Singapore. e-mail: tina.wong.t.l@sneec.com.sg

Received: April 1, 2020

Accepted: August 8, 2020

Published: August 31, 2020

Keywords: proliferative vitreoretinopathy; minipig; animal model

Citation: Wong CW, Busoy JMF, Cheung N, Barathi VA, Storm G, Wong TT. Endogenous or exogenous retinal pigment epithelial cells: a comparison of two experimental animal models of proliferative vitreoretinopathy. *Trans Vis Sci Tech.* 2020;9(9):46. <https://doi.org/10.1167/tvst.9.9.46>

Purpose: Proliferative vitreoretinopathy (PVR) is a blinding condition that can occur following ocular penetrating injury and retinal detachment. To develop effective therapeutics for PVR, it is imperative to establish an animal model that is reproducible, closest in anatomy to the human eye, and most representative of the human disease. We compared two in vivo models of PVR in minipig eyes to assess reproducibility and consistency.

Methods: Six minipigs underwent PVR induction with procedure A and six underwent procedure B. In both procedures, PVR was induced with vitrectomy, bleb retinal detachment, retinotomy, and injection of platelet-rich plasma. In procedure A, retinal pigment epithelial (RPE) cells were harvested from cadaveric pig eyes and injected at the end of surgery. In procedure B, native RPE cells were released into the vitreous cavity by creating a RPE detachment and scraping the RPE layer. PVR severity was graded on fundoscopic examination with a modified Silicone Study Classification System for PVR. Severe PVR was defined as stages 2 to 5.

Results: Three eyes (50%) and five eyes (83.3%) developed re-detachment of the retina from severe PVR in procedures A and B, respectively ($P = 0.55$). Median PVR stage was higher in eyes that underwent procedure B compared to eyes that underwent procedure A, although the difference was not statistically significant (2.5 vs. 1.5, $P = 0.26$).

Conclusions: This new model utilizing native RPE cells achieved a high consistency in inducing severe PVR in the minipig.

Translational Relevance: Our model closely follows pathogenic events in human PVR, making it ideal for preclinical testing of novel therapeutics for PVR.

Introduction

Proliferative vitreoretinopathy (PVR) is a blinding condition that can occur secondary to penetrating ocular trauma or retinal detachment or following surgery for retinal detachment repair. In these conditions, a breach in the integrity of the retina introduces macrophages, retinal pigment epithelial (RPE) cells,

glial cells, and fibroblasts into the vitreous, where they proliferate and incite inflammation. This process has been likened to keloidal scar formation, but in the eye it can result in massive retinal detachment, scarring, and obliteration of vision.¹ PVR is the most common reason for failure of retinal detachment (RD) surgery. Anatomical success rates for RD complicated by PVR are only 69% to 75% compared to 98% in RD without PVR, and visual outcomes of this surgery are worse

when complicated by PVR.^{2,3} Although surgery is the mainstay of treatment for PVR, multiple surgeries are frequently required to eventually achieve final retinal attachment with unsatisfactory visual outcomes.³ In addition, following surgery for retinal detachment, patients with PVR require twice as many resources to care for them compared to patients without PVR.³

For the past 40 years, many pharmacologic agents have shown promising results in animal models of PVR, but none has made it to routine clinical application due to limited efficacy in humans. This failure to translate preclinical success can be attributed to the fact that PVR is a multifactorial disease, parts of which are still unclear. These animal models may each be simulating particular pathways in the pathogenesis of PVR and, in doing so, may have involved pathways that are not present in human PVR pathogenesis or missed critical pathways altogether.⁴

To develop effective therapeutics for PVR, it is imperative to establish an animal model that is most representative of the human disease. In our previous study, we attempted to create a rabbit model of PVR by combining vitrectomy, retinotomy, cryotherapy, and injection of platelet-rich plasma; however, this model produced inconsistent results. Out of 11 eyes, only five developed clinically significant PVR with retinal detachment,⁵ and in most of these eyes clinical observation was hindered by the development of varying degrees of cataract.

An ideal animal model of PVR should have an anatomy and physiology that are as close to the human eye as possible. Minipigs have several advantages as an animal model of ocular disease and are increasingly being used as a substitute for nonhuman primates due to the close similarity of their eyes to the human eye. First, the size of the minipig eye and lens most closely approximates that of a human eye. Second, the intraocular distribution of melanin is most similar to the human eye, which is important when considering pharmacokinetic studies, as drug compounds often bind to melanin. Third, the vitreous humor of the minipig has a composition similar to that of the human vitreous, thus making it ideal for testing retinal therapeutics. Fourth, the smaller crystalline lens of the minipig eye reduces the likelihood of iatrogenic cataract formation following surgical intervention that may interfere with retinal examination. Finally, the retina of the minipig is very similar to that of a human. The retinal vasculature is holangiotic, and there is no tapetum lucidum in the minipig eye. Although there is no macula, minipig eyes have a visual streak containing a high density of cone photoreceptors, like the human fovea.

The first major step toward creating a PVR model that was closest to the human disease was made by García-Layana et al.⁶ in 1997. Their group was the first to switch animal species to the pig model to capitalize on the pig's anatomical similarities with the human eye. In addition, they demonstrated that the injection of external cells was not necessary to induce PVR, which was revolutionary at that time when most believed that fibroblast injection was essential for PVR to develop, a thinking that made models of that time very distant from clinical reality. Their work effectively demonstrated that endogenous cells, together with growth factors, plasma components, and their interaction with platelet derived growth factor, can induce PVR similar to the human disease. We aim to build upon this work and leverage subsequent advancements in our understanding of PVR pathogenesis to develop a minipig model of PVR that is consistent with and similar to the human disease. In this study, we compare two surgical models of PVR in the minipig eye, using exogenous or native retinal pigment epithelial cells⁷ to induce PVR disease process.

Methods

The SingHealth Institute Animal Care and Use Committee gave approval for this study (#2017/SHS/1328). All procedures were conducted in accordance with the ARVO Statement for the Use of Animals in Ophthalmic and Vision Research. Twelve eyes of 12 Gottingen minipigs were used for this study. Age range was 8 to 14 months, and average weight was 20 kg. The minipigs were anesthetized with intraperitoneal injection of ketamine hydrochloride (35–50 mg/kg) and Xylazil (5–10 mg/kg) prior to induction of PVR. Topical anesthesia (proparacaine hydrochloride 0.5%) was applied, and pupils were dilated with tropicamide 1%. Six pigs underwent procedure A and six pigs underwent procedure B, as described below.

Platelet-Rich Plasma Preparation

In both procedures, platelet-rich plasma (PRP) was prepared from minipig homologous blood 30 minutes prior to surgery, according to the method of Constable et al.⁸ Arterial blood was transferred from the minipig's ear artery into citrate blood tubes (1 part 3.8% sodium citrate to 9 parts whole blood). The blood was centrifuged at 1200 rotations per minute for 10 minutes, and the upper third of the supernatant PRP was aspirated. Platelet counts were performed on an automated Coulter counter to achieve 600,000

platelets/mm³, and 0.1 mL of PRP was injected into the vitreous cavity at the end of surgery.

Procedure A

RPE Isolation

RPE cells were isolated from cadaveric pig eyes using the methodology described by Sonoda et al.⁹ RPE cells were harvested 30 minutes before use to ensure viability of the injected cells. The RPE cell clusters were kept on ice in Dulbecco's Modified Eagle's Medium (DMEM) just before use.

Induction of PVR

PVR was induced based on a modified methodology of Umazume et al.⁷ Three-port valved 25-gauge pars plana vitrectomy (CONSTELLATION; Alcon, Geneva, Switzerland) was performed 3 mm from the limbus, taking care to avoid traumatizing the lens. First, posterior vitreous detachment was induced by suction, followed by core vitrectomy and shaving of the peripheral vitreous. Then, inferior retinal detachment was induced by injecting balanced salt solution (BSS; Alcon) into the subretinal space with a 39-gauge angled cannula. Subretinal injections were performed in the inferior retinal hemisphere at least 1 disc diameter away from the optic disc, avoiding any visible blood vessels. A retinotomy of 3 disc diameters was created within the inferiorly detached retina using the vitrector. If bleeding occurred, infusion pressure was increased to 60 mm Hg to achieve hemostasis. Finally, RPE cells (8×10^4 cells) in 0.1 mL of DMEM and PRP were injected into the vitreous cavity. The modifications from the methodology of Umazume et al.⁷ included the following: (1) we used 25-gauge vitrectomy instead of 20-gauge; (2) we created an inferior retinal detachment instead of a total retinal detachment; and (3) we created retinotomies of 3 disc diameters and injected PRP, steps that were not performed in the previously described methodology. These modifications were made to minimize the differences between procedures A and B, such that the procedures would differ mainly on the basis of exogenous RPE injection versus release of endogenous RPE cells.

Procedure B

With the exception of exogenous RPE cell isolation, the initial steps were similar to procedure A. Briefly, three-port valved 25-gauge pars plana vitrectomy (CONSTELLATION; Alcon) was performed

3 mm from the limbus. Posterior vitreous detachment was induced followed by core vitrectomy and shaving of the peripheral vitreous. The following steps differentiate the two procedures: RPE detachment was induced by injecting BSS (Alcon) into the sub-RPE space using a 39-gauge angled cannula. Inducing a RPE detachment allowed easier access to the sub-RPE space compared to inducing retinal detachment as was done in procedure A. RPE detachment is distinct from retinal detachment and can be detected on direct visualization. A retinotomy of 3 disc diameters was created within this area of RPE detachment with the vitrector. A 39-gauge angled cannula was then advanced into the sub-RPE space to scrape the RPE and dislodge these cells into the vitreous cavity (Fig. 1; Supplementary Movie S1). The release of RPE cells into the vitreous cavity simulates the process that occurs in human PVR, in which RPE cells escape from the subretinal space into the vitreous cavity through a retinal break. A 90% fluid air exchange was performed to disrupt any remaining vitreous and to extend the PVD to the peripheral retina so as to allow RPE cells to settle onto the inferior retinal surface. Air was used instead of gas, as it is short lasting and would avoid the problems of postoperative formation of gas cataract or poor visualization.

For both procedures, topical tobramycin was administered four times a day for 5 days after induction of PVR.

Investigations and Examination

The retina was examined with an indirect ophthalmoscope through a +20-diopter (D) fundus lens on days 1, 7, 14, 21, and 28 by two double-masked ophthalmologists. The choice of PVR classification is crucial to evaluating an animal model in terms of how representative the model is of the human disease. Classification systems for animal models of PVR were mainly developed for rabbits, including the Fastenberg classification,¹⁰ which was designed for intact vitreous PVR models, and the revised PVR classification,¹¹ which was proposed for a vitrectomized model/cell intravitreal injection model. In this study, we opted to use a modified version of the Silicon Study Classification System, a classification of human PVR, which was also employed by Umazume's group⁷ in their description of a swine model of PVR:

- Stage 0—Normal retina, retinal or vitreous pigment clumps
- Stage 1—Inner retinal wrinkling
- Stage 2—Retinal detachment, 1 quadrant (1–3 clock hours)

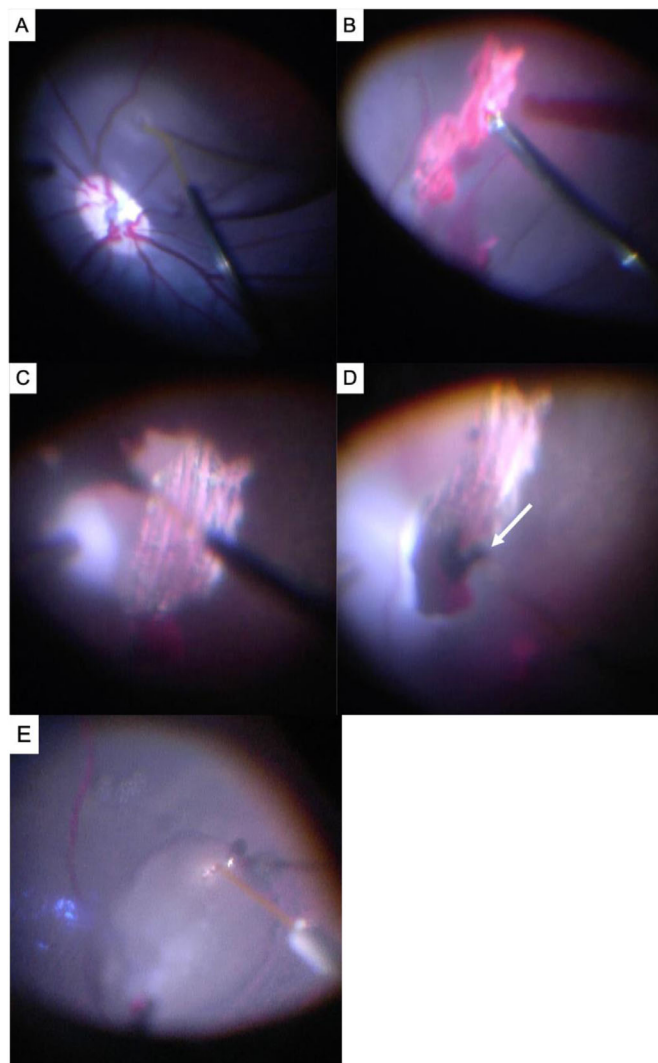


Figure 1. Intraoperative photographs of the surgical steps. (A) After posterior vitreous detachment and vitrectomy, a 39-gauge angled cannula was advanced into the sub-RPE space. BSS was slowly infused into the sub-RPE space to create a RPE detachment. (B) A large retinotomy was created with the vitrector in a radial fashion to avoid transecting large blood vessels. (C) The RPE was scraped with an angled cannula to dislodge it from the retina. (D) Large clumps of RPE cells (*arrow*) were released into the vitreous cavity. (E) Induction of retinal detachment in procedure A is shown.

Stage 3—Retinal detachment, 2 quadrants (4–6 clock hours)

Stage 4—Retinal detachment, 3 quadrants (7–9 clock hours)

Stage 5—Retinal detachment, 4 quadrants (10–12 clock hours)

Severe PVR was defined as retinal re-detachment, or stages 2 to 5. Fundus photography and spectral-domain optical coherence tomography (SD-OCT) were performed (Spectralis OCT; Heidelberg Engineering, Heidelberg, Germany). At the end of study, minipigs

were euthanized with intraperitoneal pentobarbitone (60–150 mg/kg) and study eyes were enucleated.

Collection of Vitreous Samples and Analysis

Vitreous humor samples of at least 0.2 mL were obtained at the start of the vitrectomy procedure with the vitrector attached to a 3-mL syringe. On day 28, eyes were enucleated and the vitreous obtained prior to paraffin fixation of the eye. Vitreous samples were stored at -80°C prior to analysis. The vitreous concentrations of interleukin 6 (IL-6), C-reactive protein (CRP), platelet-derived growth factor BB (PDGF-BB), and vascular endothelial growth factor (VEGF) were determined using a human multiplex enzyme-linked immunosorbent assay kit (AYOXXA, Köln, Germany).

Histopathology and Immunohistochemistry

Minipig eyes were fixed in a mixture of 10% neutral buffered formalin solution (Leica Surgipath; Leica Biosystems, Wetzlar, Germany) for 24 hours. The whole eye was then dissected to anterior and posterior segments prior to dehydration in increasing concentrations of ethanol, clearance in xylene, and embedding in paraffin (Surgipath; Leica Biosystems). Four-micron sections were cut with a rotary microtome (RM2255; Leica Biosystems) and collected on POLYSINE microscope glass slides (Thermo Fisher Scientific, Waltham, MA). The sections were dried in an oven at 37°C for at least 24 hours. The sections were then heated on a 60°C heat plate, deparaffinized in xylene, and rehydrated in decreasing concentrations of ethanol in preparation for staining. A standard procedure for hematoxylin and eosin (H&E) staining was performed. A light microscope (Axioplan 2; Carl Zeiss Meditec, Jena, Germany) was used to examine the slides, and images were captured.

For immunofluorescence staining, heat-induced antigen retrieval was performed by incubating sections in sodium citrate buffer (10-mM sodium citrate, 0.05% Tween-20, pH 6.0) for 20 minutes at 95°C to 100°C . The sections were then cooled down in sodium citrate buffer for 20 minutes at room temperature and washed three times for 5 minutes each with $1\times$ phosphate-buffered saline (PBS). Non-specific sites were blocked with blocking solution of 5% bovine serum albumin (BSA) in 0.1% Triton X-100 and $1\times$ PBS for 1 hour at room temperature in a humidified chamber. The slides were then rinsed briefly with $1\times$ PBS. A specific primary antibody shown in Table 1 was applied and incubated overnight at 4°C in a humidified chamber prepared in blocking solution. After washing twice with $1\times$ PBS

Table 1. Antibodies Used for Immunohistochemical Staining.

Antibody	Catalog No.	Company	Concentration
Smooth muscle actin	710487	Thermo Fisher Scientific	1:200
Cytokeratin	MA513156	Thermo Fisher Scientific	1:200

and once with $1 \times$ PBS with 0.1% Tween-20 for 10 minutes each, Alexa Fluor 488 conjugated fluorescein-labeled secondary antibody (Thermo Fisher Scientific) was applied at a concentration of 1:1000 in blocking solution and incubated for 90 minutes at room temperature. To visualize cell nuclei, the slides were then washed twice with $1 \times$ PBS and once with $1 \times$ PBS with 0.1% Tween-20 for 5 minutes each, and ProLong Diamond Antifade Mountant (Thermo Fisher Scientific) was used. For negative controls, primary antibody was omitted.

A fluorescence microscope (Axioplan 2; Carl Zeiss Meditec) was used to examine the slides, and images were captured. Experiments were repeated in duplicate for each antibody.

Statistics

Two-sided χ^2 analysis was used to compare the proportion of eyes with severe PVR in each group. Student's *t*-test was used to compare cytokine levels between the groups, and Mann-Whitney U test was used to compare median PVR stage. Statistical significance was set at $P = 0.05$ and Stata 16.0 (StataCorp, College Station, TX) was used for the analysis.

Results

PVR Staging

On day 28, for procedure A, three eyes (50%) developed re-detachment of the retina due to severe PVR (Figs. 2, 3). Three eyes developed PVR stage 1, one eye developed PVR stage 2, and two eyes developed PVR stage 5. For procedure B, five eyes (83.3%) had retinal re-detachment due to severe PVR. One eye developed stage 1 PVR, two eyes developed stage 2 PVR, one eye developed stage 3 PVR, and two eyes developed stage 5 PVR. There was no statistically significant difference in median PVR stage (1.5 vs. 2.5; $P = 0.26$) or proportion of severe PVR ($P = 0.55$).

Cytokine and Growth Factor Levels

Mean levels of inflammatory cytokines and growth factors were, in general, higher for procedure B than for

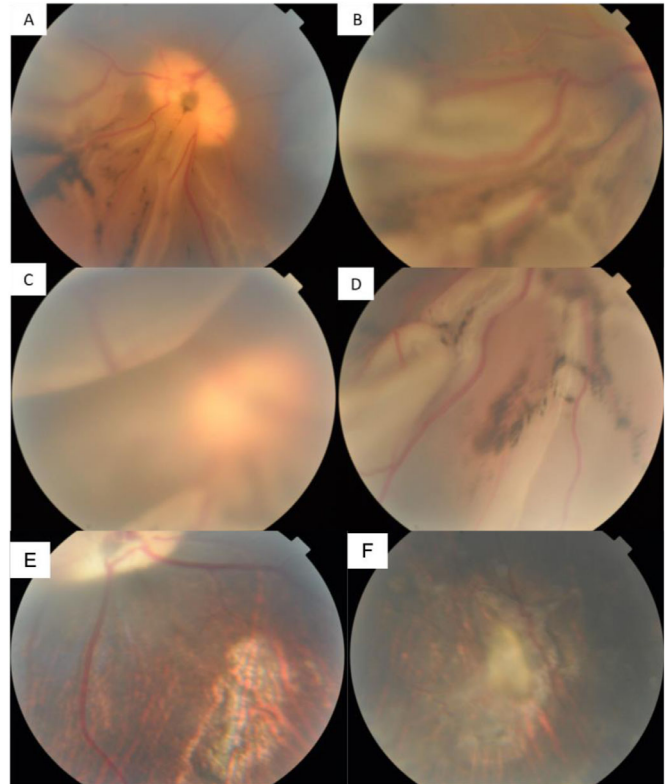


Figure 2. Fundus photographs at day 14 (A, B) and day 28 (C, D) of an eye with stage 5 PVR. On day 14, there was detachment of the inferior and temporal retina (A). Retinal folds and deposits of RPE cells can be seen on the retinal surface (B). On day 28, the retinal detachment had progressed to involve the entire retina (C). Fixed retinal folds associated with RPE cells can be observed in the inferior retina. (E) An eye with reattachment of the retina. (F) RPE atrophy can be seen surrounding a fibrotic retinal scar.

procedure A (Table 2), including CRP, IL-6, PDGF-BB, and VEGF-A, but they did not reach statistical significance.

Histology and Immunohistochemistry

H&E staining demonstrated folding of the inner retina, characteristic of PVR (Figs. 4A, 4B). Alpha smooth muscle actin, a marker for myofibroblasts derived mainly from dedifferentiated RPE cells, was observed on epiretinal membranes (Fig. 4C). Cytokeratin-positive spindle cells can be seen within fibrocellular membranes associated with these retinal folds (Fig. 4D).

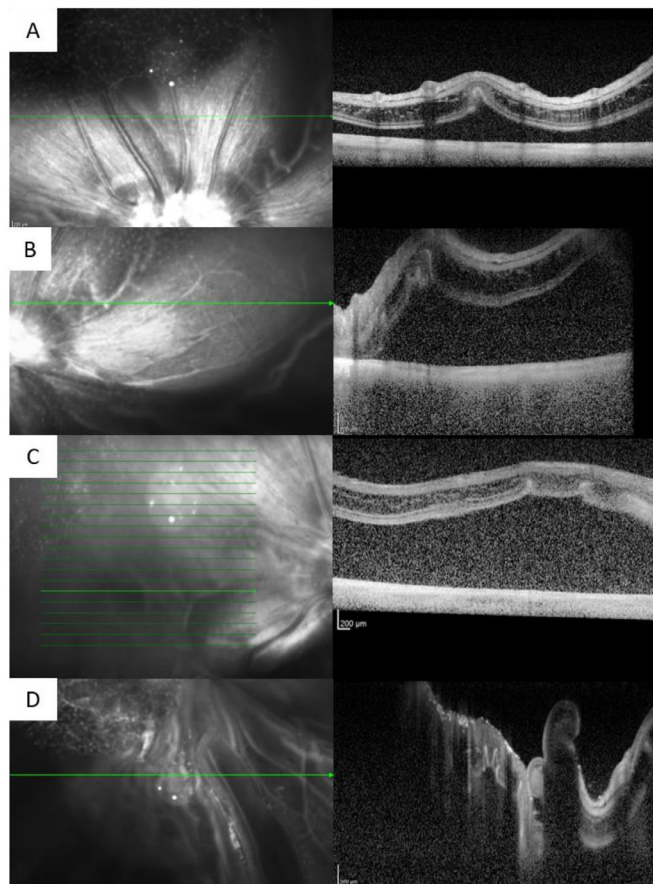


Figure 3. OCT scans of the same eye on day 28. Green lines on the red-free images (left) represent the scanned segments. These scans confirm the presence of retinal detachment in the superior (A), temporal (B), nasal (C), and inferior (D) retina. Folds in the inferior retina (D) can be seen. These folds resulted from traction exerted by PVR membranes.

Table 2. Cytokine and Growth Factor Levels at Week 4

Cytokine (pg/mL)	Procedure A	Procedure B	<i>P</i>
IL-6	1.0 ± 1.5	1.7 ± 1.9	0.53
CRP	27.0 ± 33.3	50.1 ± 20.4	0.19
PDGF-BB	5.2 ± 5.9	20.0 ± 16.3	0.21
VEGF-A	783.9 ± 848.2	895.6 ± 554.3	0.87

Discussion

To the best of our knowledge, this is the first study to compare two surgical animal models of PVR in the minipig: injection of exogenous RPE cells (procedure A) versus in situ release of endogenous RPE cells (procedure B). Procedure B was designed to more closely follow and reflect the pathogenic events in clinical PVR. We observed higher rates of severe PVR, as well as higher concentration of inflammatory cytokines and growth factors associated with PVR,

with this model, although statistical significance was not reached. A larger study is required to validate these findings.

Different animal species have been used to model PVR, each with its own pros and cons.¹² For example, rabbit models have the advantage of large vitreous volume and relative ease of manipulation with less risk of damage to the lens and retina compared to smaller animals such as the rat. However, their retinal structure, including blood vessels and nerve fiber distribution, differs from that of humans, complicating direct comparison to the human disease in anatomic and pathologic terms. Rodent models are less commonly employed. Although murine species are relatively easier to modify genetically, their large crystalline lens and small vitreous volume severely limit the feasibility of surgical manipulation and fundus examinations.^{13,14} Pig models are rarely used but are increasingly being recognized as an ideal substitute for nonhuman primate models.^{6,7} Their eyes are similar in size to the human eye, their retinæ are holangiotic like the human eye, and they have a cone-enriched area centralis that is similar to the human fovea. In this study, we have shown that PVR that closely follows the pathogenesis of the human disease (i.e., development of fibrotic membranes and tractional retinal detachment following exposure of RPE cells to the vitreous cavity) can be successfully induced in minipig eyes.

Most animal models of PVR do not replicate the pathogenic processes in the human disease. Such models rely on the addition of cells or growth factors associated with the pathogenesis of PVR and may or may not include other interventions to disrupt the vitreous, such as with gas injection or vitrectomy.⁴ In vivo models in which PVR is induced by intravitreal injection of fibroblasts,¹⁵ RPE cells,^{7,16–25} or macrophages²⁶ introduce large quantities of exogenous cells that do not naturally occur even in the disease state. More importantly, they do not account for key steps in PVR development, such as cellular survival, epithelial mesenchymal transformation, and proliferation.⁴ Therapeutic agents that are seemingly efficacious in these models may be affecting the injected cells directly rather than inhibiting the endogenous PVR cascade, resulting in falsely promising results. In particular, the fibroblast injection model is inherently flawed because dermal, corneal, or conjunctival fibroblasts are not involved in the pathogenesis of human PVR.

Injection models utilizing cultured RPE cells and macrophages are more relevant to human disease.^{13,26} However, the macrophage injection model does not expose RPE cells, which are thought to play a critical role in the development of human PVR.⁴ In addition

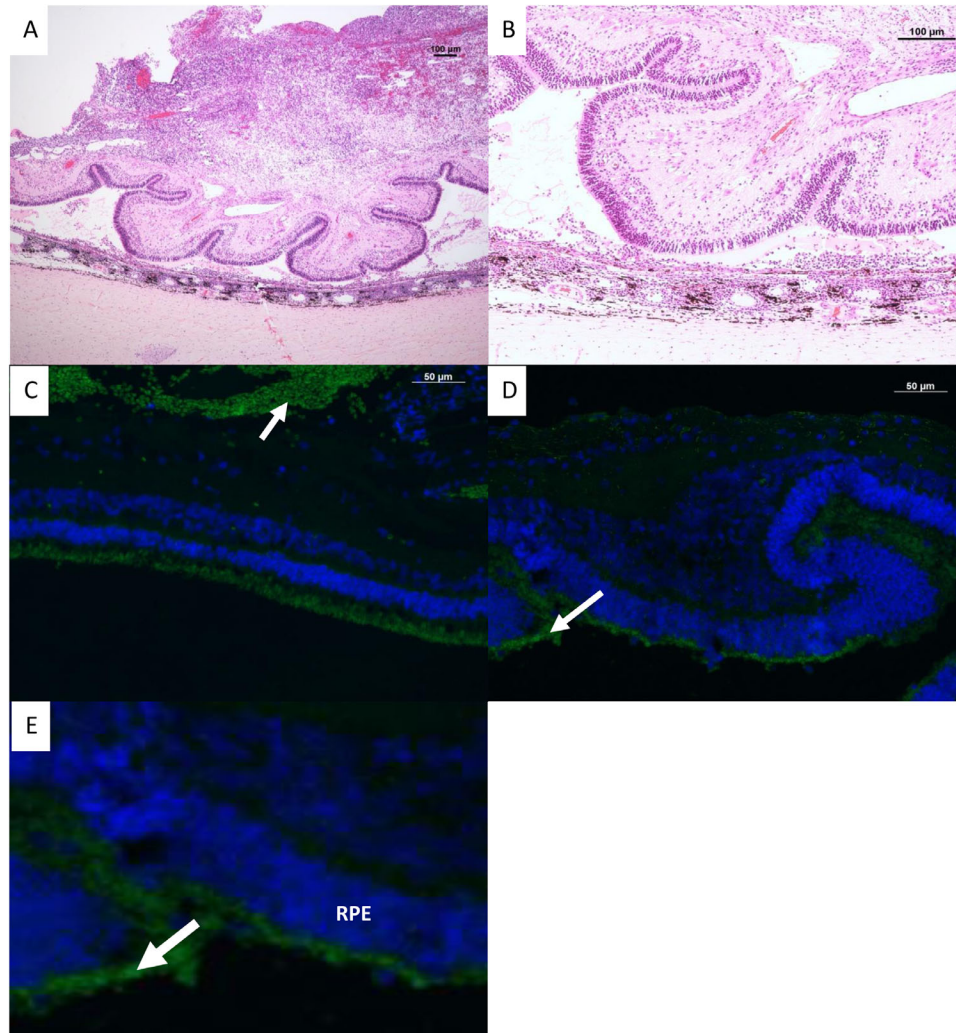


Figure 4. Histopathological staining of the retina in an eye with PVR. (A) H&E stain at 10× magnification demonstrating folding of the detached retina. (B) The same H&E stain at 20× magnification. (C) Immunohistochemical staining showing the presence of alpha smooth muscle actin on epiretinal membranes (*arrow*) and positive cytokeratin staining on subretinal membranes (D, *arrow*). (E) Magnified view of positive cytokeratin staining (*arrow*) of a membrane on the RPE layer.

to RPE cells, glial elements such as microglia and Müller cells play an equally important role in promoting retinal remodeling, leading to retinal shortening within the neurosensory retina while interacting with macrophages and RPE cells in the subretinal space to form subretinal membranes.⁴ The relationship between macrophages and cells from the neuroretina (e.g., RPE and glial cells) warrants further investigation. Exogenous RPE cells (Table 3) are useful in animal models of PVR because it is difficult to release endogenous RPE cells in sufficient quantity to trigger the PVR process.¹² Umazume et al.⁷ described a porcine model of PVR in which injection of cadaveric porcine RPE cells successfully induced severe PVR in 14 out of 14 eyes after 14 days. However, exogenous RPE cell injections have a few issues, including the difficulty of keeping these cells viable, the risk of infection, and the possibility

that these exogenous cells may trigger an immune-mediated rejection response.¹⁶ The excessive inflammation induced by the rejection response may detract from the actual PVR process and overestimate the treatment effect of anti-inflammatory therapeutics on PVR. To avoid these problems, we have developed a model of PVR using exclusively endogenous RPE cells. This is possible in the surgical model we described by inducing a RPE detachment and then accessing the RPE through a retinotomy. With this technique, we were able to consistently release a large quantity of RPE cells into the vitreous cavity. Our observation of a higher re-detachment rate and higher concentration of growth factors related to the later proliferative stage of PVR in procedure B may suggest the availability of a larger quantity of free-floating and viable endogenous RPE cells in the vitreous cavity compared to procedure A,

Table 3. Summary of In Vivo PVR Models Utilizing Injection of Retinal Pigment Epithelial Cells

PVR Models	Year	Animal	Summary of Procedure	Reported PVR Induction Rate
Pure injection				
Autologous RPE cell injection ²³	1981	Rabbit	Injection of autologous RPE cells harvested from enucleated fellow eye	86%
Homologous RPE cell injection ¹⁹	1982	Rabbit	Injection of rabbit RPE without vitrectomy	100%
Heterologous RPE cell injection ^{16,18,25}	1987	Rabbit	Injection of human, bovine, or rat RPE cells without vitrectomy	75%
Homologous RPE cells + PDGF-BB injection ²⁰	2015	Rabbit	Pars plana removal of 0.2 mL vitreous, injection of RPE cells and PDGF-BB	100%
Vitreous compression + injection				
Gas compression + homologous RPE injection ^{21,22}	2002	Rabbit	Perfluorocarbon or sulfur hexafluoride gas injection followed by injection of rabbit RPE cells 7–10 days later	72.7%
Gas compression vitrectomy + homologous RPE cell + PDGF-BB injection ¹⁷	2007	Rabbit	Perfluoropropane gas injection followed by gas–fluid exchange, injection of rabbit RPE cells and PDGF-BB.	Most animals
Mechanical vitrectomy + injection				
Vitrectomy + artificial RD + RPE cell injection ^{7,24}	2012	Swine	Pars plana vitrectomy followed by subretinal injection to induce retinal detachment followed by intravitreal injection of porcine RPE cells	100%

where the number of viable exogenous RPE cells may have been much lower.

The dispase injection model described by Frenzel et al.²⁷ is an interesting model in which an intravitreal injection of dispase in the rabbit eye was sufficient to induce PVR in all eyes. Dispace cleaved basement membrane, allowing RPE cells to be released into the vitreous cavity without the need for a retinal break. This allowed PVR induction in a relatively inexpensive, technically easy way, eliminating the use of surgical equipment and introduction of exogenous cells. However, a major problem with this model was the formation of cataract and zonular dehiscence, presumably due to the effect of dispase on type IV collagen in the lens capsule. This was demonstrated by Kralinger et al.,²⁸ who found a reproducibility of 87% in PVR induction, but 90% of eyes developed severe cataract, and lens luxation occurred in 47% of these eyes. In this model, dispase was not washed out of the eye, raising the question of whether the PVR process was triggered as a result of a toxic reaction to dispase.

Injection of PRP simulates the situation in human PVR where patients with vitreous hemorrhage and retinal detachment concurrently tend to be at high risk

of PVR.^{6,29} The increased risk of PVR arises from the high concentrations of growth factors within the vitreous cavity which result in a conducive environment for survival and epithelial–mesenchymal transition of liberated RPE cells within the vitreous. However, injecting whole blood into the vitreous cavity obstructs visualization of the retina. Injecting PRP retains the necessary growth factors while avoiding the problem of poor visualization and inaccurate PVR classification.

There are some limitations to our model. First, we did not find a statistically significant difference between the two models in the proportion of eyes with severe PVR. This is likely due to the small sample size, but even with these small numbers we demonstrated that the use of endogenous cells was at least as reproducible for PVR induction as using exogenous cells, with the added advantage of eliminating the time-consuming and expensive step of harvesting RPE cells from cadaveric eyes. Second, surgical models are relatively expensive, requiring equipment for vitrectomy and a surgical microscope, as well as surgical expertise. It is technically difficult to operate on a pig's eye, and there is a learning curve to creating a RPE detachment. However, considering the cost of phase 1 or 2 human

clinical trials, it is far more cost effective to evaluate potential therapeutics in an accurate preclinical disease model. Third, scraping of RPE cells may cause more trauma to the retina than performing a simple retinal detachment, but this is not visually evident in terms of retinal tearing or increased bleeding. It is also difficult to quantify if either procedure may cause more inflammation, because the possible additional trauma induced by scraping RPE cells may or may not be more than the inflammation caused by a possible rejection of exogenous RPE cells. Our study was designed to assess exogenous and endogenous RPE cell release models and not to determine if one procedure was more aggressive than the other. Fourth, we performed an air–fluid exchange in procedure B, whereas this step was not performed in procedure A. Fluid–air exchange is a common procedure performed during vitrectomy in human patients for various indications. It is short lasting and does not generally cause gas cataract, even in human patients with clear crystalline lenses, like a long-acting gas would. We did not notice the formation of gas cataract in any of the eyes that underwent procedure B.

In conclusion, we have demonstrated a consistent model of PVR in the minipig that can be surgically induced using native RPE cells. This may be a suitable model for both understanding the pathogenesis of PVR and for testing novel therapeutics to treat PVR.

Acknowledgments

Supported by funding from the National Medical Research Council, Singapore (NMRC/FLWSHP/045/2017-00), and by the SingHealth Duke–NUS Ophthalmology & Visual Sciences Academic Clinical Programme, Singapore (R1484/67/2017).

Disclosure: **C.W. Wong**, None; **J.M.F. Busoy**, None; **N. Cheung**, None; **V.A. Barathi**, None; **G. Storm**, None; **T.T. Wong**, None

References

1. Newsome DA, Rodrigues MM, Machemer R. Human massive periretinal proliferation. In vitro characteristics of cellular components. *Arch Ophthalmol*. 1981;99:873–880.
2. Wong CW, Wong WL, Yeo IY, et al. Trends and factors related to outcomes for primary rhegmatogenous retinal detachment surgery in a large Asian tertiary eye center. *Retina*. 2014;34:684–692.
3. Patel NN, Bunce C, Asaria RH, Charteris DG. Resources involved in managing retinal detachment complicated by proliferative vitreoretinopathy. *Retina*. 2004;24:883–887.
4. Pastor JC, Rojas J, Pastor-Idoate S, Di Lauro S, Gonzalez-Buendia L, Delgado-Tirado S. Proliferative vitreoretinopathy: a new concept of disease pathogenesis and practical consequences. *Prog Retin Eye Res*. 2016;51:125–155.
5. Wong CW, Cheung N, Ho C, Barathi V, Storm G, Wong TT. Characterisation of the inflammatory cytokine and growth factor profile in a rabbit model of proliferative vitreoretinopathy. *Sci Rep*. 2019;9:15419.
6. García-Layana A, Pastor JC, Saornil MA, Gonzalez G. Porcine model of proliferative vitreoretinopathy with platelets. *Curr Eye Res*. 1997;16:556–563.
7. Umazume K, Barak Y, McDonald K, Liu L, Kaplan HJ, Tamiya S. Proliferative vitreoretinopathy in the Swine—a new model. *Invest Ophthalmol Vis Sci*. 2012;53:4910–4916.
8. Constable IJ, Oguri M, Chesney CM, Swann DA, Colman RW. Platelet-induced vitreous membrane formation. *Invest Ophthalmol*. 1973;12:680–685.
9. Sonoda S, Spee C, Barron E, Ryan SJ, Kannan R, Hinton DR. A protocol for the culture and differentiation of highly polarized human retinal pigment epithelial cells. *Nat Protoc*. 2009;4:662–673.
10. Fastenberg DM, Diddie KR, Dorey K, Ryan SJ. The role of cellular proliferation in an experimental model of massive periretinal proliferation. *Am J Ophthalmol*. 1982;93:565–572.
11. Hida T, Chandler DB, Sheta SM. Classification of the stages of proliferative vitreoretinopathy in a refined experimental model in the rabbit eye. *Graefes Arch Clin Exp Ophthalmol*. 1987;225:303–307.
12. Hou H, Nudleman E, Weinreb RN. Animal models of proliferative vitreoretinopathy and their use in pharmaceutical investigations. *Ophthalmic Res*. 2018;60:195–204.
13. Lin ML, Li YP, Li ZR, Lin JX, Zhou XL, Liang D. Macrophages acquire fibroblast characteristics in a rat model of proliferative vitreoretinopathy. *Ophthalmic Res*. 2011;45:180–190.
14. Miller W, Makova KD, Nekrutenko A, Hardison RC. Comparative genomics. *Annu Rev Genomics Hum Genet*. 2004;5:15–56.
15. Algvere P, Kock E. Experimental Fibroplasia in the rabbit vitreous. Retinal detachment induced by autologous fibroblasts. *Albrecht Von Graefes Arch Klin Exp Ophthalmol*. 1976;199:215–222.
16. Wong CA, Potter MJ, Cui JZ, et al. Induction of proliferative vitreoretinopathy by a unique line of

- human retinal pigment epithelial cells. *Can J Ophthalmol*. 2002;37:211–220.
17. Agrawal RN, He S, Spee C, Cui JZ, Ryan SJ, Hinton DR. In vivo models of proliferative vitreoretinopathy. *Nat Protoc*. 2007;2:67–77.
 18. Borhani H, Peyman GA, Rahimy MH, Thompson H. Suppression of experimental proliferative vitreoretinopathy by sustained intraocular delivery of 5-FU. *Int Ophthalmol*. 1995;19:43–49.
 19. Fastenberg DM, Diddie KR, Sorgente N, Ryan SJ. A comparison of different cellular inocula in an experimental model of massive periretinal proliferation. *Am J Ophthalmol*. 1982;93:559–564.
 20. Ishikawa K, He S, Terasaki H, et al. Resveratrol inhibits epithelial-mesenchymal transition of retinal pigment epithelium and development of proliferative vitreoretinopathy. *Sci Rep*. 2015;5:16386.
 21. Kuo HK, Chen YH, Wu PC, et al. Attenuated glial reaction in experimental proliferative vitreoretinopathy treated with liposomal doxorubicin. *Invest Ophthalmol Vis Sci*. 2012;53:3167–3174.
 22. Lee JJ, Park JK, Kim YT, et al. Effect of 2'-benzoyl-oxycinnamaldehyde on RPE cells in vitro and in an experimental proliferative vitreoretinopathy model. *Invest Ophthalmol Vis Sci*. 2002;43:3117–3124.
 23. Radtke ND, Tano Y, Chandler D, Machemer R. Simulation of massive periretinal proliferation by autotransplantation of retinal pigment epithelial cells in rabbits. *Am J Ophthalmol*. 1981;91:76–87.
 24. Umazume K, Liu L, Scott PA, et al. Inhibition of PVR with a tyrosine kinase inhibitor, dasatinib, in the swine. *Invest Ophthalmol Vis Sci*. 2013;54:1150–1159.
 25. Weinsieder A, Radtke ND, Currier GJ, Caple S, Presley E, Weinsieder G. Bovine RPE heterotransplants simulate proliferative vitreoretinopathy (PVR) in rabbits. *Metab Pediatr Syst Ophthalmol (1985)*. 1987;10:2–8.
 26. Hui YN, Goodnight R, Sorgente N, Ryan SJ. Fibrovascular proliferation and retinal detachment after intravitreal injection of activated macrophages in the rabbit eye. *Am J Ophthalmol*. 1989;108:176–184.
 27. Frenzel EM, Neely KA, Walsh AW, Cameron JD, Gregerson DS. A new model of proliferative vitreoretinopathy. *Invest Ophthalmol Vis Sci*. 1998;39:2157–2164.
 28. Kralinger MT, Kieselbach GF, Voigt M, et al. Experimental model for proliferative vitreoretinopathy by intravitreal dispase: limited by zonulolysis and cataract. *Ophthalmologica*. 2006;220:211–216.
 29. Pinon RM, Pastor JC, Saornil MA, et al. Intravitreal and subretinal proliferation induced by platelet-rich plasma injection in rabbits. *Curr Eye Res*. 1992;11:1047–1055.

Supplementary Material

Supplementary Movie S1. Surgical video demonstrating the key steps of PVR induction in Procedure B.